

31.4: Cell Designs for Fast Reflective Cholesteric LCDs

X.-D. Mi, D.-K. Yang

Liquid Crystal Institute, Kent State University, Kent, OH

Abstract

We numerically study the dynamic process of transitions among textures in bistable cholesteric reflective displays, and analyze the effects of the parameters: surface anchoring, applied field, cell thickness, pitch and elastic constants. Our result shows that fast homeotropic-planar transition, essential in order to use cholesteric liquid crystals in video rate operations, can be achieved using cells with homeotropic anchoring.

Introduction

Cholesteric liquid crystals, used for reflective displays because of their bistability and reflectivity, exhibit two stable states at zero field.^{1, 2} One is the reflecting planar texture and the other is the non-reflecting focal conic texture. A cholesteric liquid crystal ($\Delta\epsilon > 0$) can be quickly switched directly from the planar texture to the focal conic texture but not vice versa.² In order to switch the cholesteric liquid crystal from the focal conic to the planar texture, it has to be first switched to the homeotropic texture and then relaxes to the planar texture. The homeotropic-planar transition is usually slow, a few hundred ms long. Because of this slow transition, the application of cholesteric liquid crystals is limited to displaying static images. To display dynamic images at video rate, it is necessary to reduce the homeotropic-planar transition time. Furthermore, this transition has played an important role in dynamic drive schemes.³ Therefore, it is greatly desired to have a complete understanding of it. There are many parameters affecting the transition: cell surface anchoring and thickness, elastic constants, intrinsic pitch, and viscosity of the liquid crystal. Examining so many parameters experimentally to obtain the fast transition would be expensive if not impossible. Therefore we simulate this dynamic process to investigate the effects of surface anchoring and material parameters. We use the results as a guidance to design cells and choose material parameters to optimize reflective cholesteric liquid crystal displays.

Numerical study

In the transition from the field-induced homeotropic texture to the planar texture of a cholesteric liquid crystal, the director \vec{n} can be approximately considered to only be a function of the coordinate z which is

chosen to be perpendicular to the liquid crystal cell. $\vec{n} = n_x(z)\hat{x} + n_y(z)\hat{y} + n_z(z)\hat{z}$. The free energy density can be derived from the derivatives of n_x , n_y and n_z . The cholesteric liquid crystal we are considering has a pitch P_o in the visible light wavelength region; the cell thickness h of a cholesteric reflective display is usually about 5 μm . $h/P_o \sim 10$ and in the planar texture, the twist angle from the bottom of the cell to the top of the cell $\Delta\phi = 2\pi h/P_o \sim 20\pi$. There is a problem in numerical calculation if \vec{n} is used directly. In programming, the discretization destroys the symmetry between \vec{n} and $-\vec{n}$. This problem is avoided by using the tensor relaxation method where we introduce the tensor $\overset{\leftrightarrow}{Q}$ ⁴

$$Q_{ij} = n_i n_j - \frac{1}{3} \delta_{ij} \quad (1)$$

Expressed in the derivatives of $\overset{\leftrightarrow}{Q}$, the Oseen-Frank free energy is

$$\begin{aligned} f = & \left(-\frac{K_{11}}{12} + \frac{K_{22}}{4} + \frac{K_{33}}{12} \right) G_1^{(2)} + \left(\frac{K_{11}-K_{22}}{2} \right) G_2^{(2)} + \left(\frac{K_{33}-K_{11}}{4} \right) G_6^{(3)} \\ & - q_o K_{22} G_4^{(2)} - \frac{1}{2} \epsilon_o \Delta\epsilon (\vec{E} \bullet \vec{n})^2 + \frac{K_{22}}{2} q_o^2 \\ & + \frac{K_{22}}{2} \nabla \bullet (\vec{n} \nabla \bullet \vec{n} + \vec{n} \times \nabla \times \vec{n}) \end{aligned} \quad (2)$$

where

$$\begin{aligned} G_1^{(2)} &= Q_{jk,l} Q_{jk,l} = 2n_{k,l} n_{k,l} = 2[(\nabla \bullet \vec{n})^2 + (\vec{n} \bullet \nabla \times \vec{n})^2 \\ &+ (\vec{n} \times \nabla \times \vec{n})^2 - \nabla \bullet (\vec{n} \nabla \bullet \vec{n} + \vec{n} \times \nabla \times \vec{n})] \end{aligned} \quad (3)$$

$$\begin{aligned} G_2^{(2)} &= Q_{jk,l} Q_{jl,l} = n_{k,k} n_{l,l} + n_{k,n_j} n_{j,k} n_{j,l} \\ &= (\nabla \bullet \vec{n})^2 + (\vec{n} \times \nabla \times \vec{n})^2 \end{aligned} \quad (4)$$

$$G_4^{(2)} = e_{jkl} Q_{jm} Q_{km,l} = e_{jkl} n_j n_{k,l} = -\vec{n} \bullet \nabla \times \vec{n} \quad (5)$$

$$\begin{aligned} G_6^{(3)} &= Q_{jk} Q_{lm,j} Q_{lm,k} = 2(n_{k,n_j} n_{j,k} n_{j,l} - \frac{1}{3} n_{k,l} n_{k,l}) \\ &= -\frac{2}{3}(\nabla \bullet \vec{n})^2 - \frac{2}{3}(\vec{n} \bullet \nabla \times \vec{n})^2 + \frac{4}{3}(\vec{n} \times \nabla \times \vec{n})^2 \\ &+ \frac{2}{3}\nabla \bullet (\vec{n} \nabla \bullet \vec{n} + \vec{n} \times \nabla \times \vec{n}) \end{aligned} \quad (6)$$

The last term in Eq. (2) is a surface term and can be neglected because the fixed boundary condition (strong anchoring) is used in our calculation. The dynamic equations are

$$\gamma \frac{dn_i}{dt} = -\frac{\delta[f - \lambda(\vec{n}^2 - 1)]}{\delta n_i} = -\frac{\delta f}{\delta n_i} + 2\lambda n_i = -\frac{\delta f}{\delta Q_{ik}} \frac{\partial Q_{ik}}{\partial n_i} + 2\lambda n_i, \quad (7)$$

where λ is the Lagrange multiplier due to the constraint that $\vec{n}^2 = 1$. Using Eq. (7), we calculate \vec{n} as a function of time. The quantities of interest are the polar angle θ given by

$$\sin \theta = \sqrt{n_x^2(z) + n_y^2(z)} \quad (8)$$

and the normalized twisting rate S defined by

$$S = \frac{1}{q_o} (-\vec{n} \bullet \nabla \times \vec{n}) = \frac{1}{q_o} \sin^2 \theta \frac{\partial \phi}{\partial z} \quad (9)$$

where ϕ is the azimuthal angle and q_o is the chirality of the liquid crystal. The optical reflection is determined by S .

Report Documentation Page			<i>Form Approved OMB No. 0704-0188</i>	
Public reporting burden for the collection of information is estimated to average 1 hour per response, including the time for reviewing instructions, searching existing data sources, gathering and maintaining the data needed, and completing and reviewing the collection of information. Send comments regarding this burden estimate or any other aspect of this collection of information, including suggestions for reducing this burden, to Washington Headquarters Services, Directorate for Information Operations and Reports, 1215 Jefferson Davis Highway, Suite 1204, Arlington VA 22202-4302. Respondents should be aware that notwithstanding any other provision of law, no person shall be subject to a penalty for failing to comply with a collection of information if it does not display a currently valid OMB control number.				
1. REPORT DATE 1998	2. REPORT TYPE	3. DATES COVERED 00-00-1998 to 00-00-1998		
4. TITLE AND SUBTITLE Cell Designs for Fast Reflective Cholesteric LCDs		5a. CONTRACT NUMBER		
		5b. GRANT NUMBER		
		5c. PROGRAM ELEMENT NUMBER		
6. AUTHOR(S)		5d. PROJECT NUMBER		
		5e. TASK NUMBER		
		5f. WORK UNIT NUMBER		
7. PERFORMING ORGANIZATION NAME(S) AND ADDRESS(ES) Liquid Crystal Institute,Kent State University,Kent ,OH,44242-0001		8. PERFORMING ORGANIZATION REPORT NUMBER		
9. SPONSORING/MONITORING AGENCY NAME(S) AND ADDRESS(ES)		10. SPONSOR/MONITOR'S ACRONYM(S)		
		11. SPONSOR/MONITOR'S REPORT NUMBER(S)		
12. DISTRIBUTION/AVAILABILITY STATEMENT Approved for public release; distribution unlimited				
13. SUPPLEMENTARY NOTES				
14. ABSTRACT				
15. SUBJECT TERMS				
16. SECURITY CLASSIFICATION OF:		17. LIMITATION OF ABSTRACT	18. NUMBER OF PAGES	19a. NAME OF RESPONSIBLE PERSON
a. REPORT unclassified	b. ABSTRACT unclassified		c. THIS PAGE unclassified	4

Results of simulation

In our simulation, the liquid crystal is initially in the homeotropic texture under an applied electric field higher than $E_c = \frac{\pi^2}{P_o} \sqrt{\frac{K_{22}}{\epsilon_0 \Delta \epsilon}}$. When the electric field is turned off, some small random noise is superimposed on the initial state, and the liquid crystal relaxes to the planar texture. We first study the effects of surface anchoring on the homeotropic-planar relaxation. The director configurations in the relaxation are shown in Figs. 1(a) and (b) for cells with homogeneous and homeotropic anchoring, respectively. (For the purpose of illustration, the cell thickness h for Fig. 1 is chosen to be $4P_o$, instead of $10P_o$, which is the value close to that of a real cholesteric display cell). For the cell with homogeneous anchoring, in the final state given by our simulation, the pitch of the liquid crystal is $P=h/2$ instead of the intrinsic pitch $P_o=h/4$. This is the transient planar texture and is metastable. The liquid crystal will further relax to the stable planar texture with the intrinsic pitch P_o . This relaxation is a slow nucleation process initiated by defects. Experimental studies show that the transition from the transient planar texture to the stable planar texture is usually a few hundreds ms long. Our model does not include defects and does not give the transition from the transient planar texture to the stable planar texture. For the cell with homeotropic anchoring, the final state given by our simulation has the pitch $P=h/3.5$ which is much closer to the intrinsic pitch $P_o=h/4$.

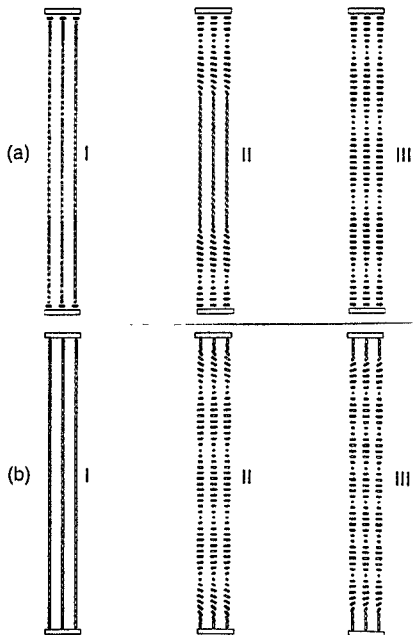


Fig.1 Director configurations in the homeotropic-planar transition. (I) initial state, (II) intermediate state and (III) final state. (a) cell with homogeneous anchoring, (b) cell with homeotropic anchoring.

We study the homeotropic-planar relaxation in cells of the thickness $h=10P_o=5 \mu\text{m}$ and investigate how the relaxation takes place. We use the parameters: elastic constants $K_{11}=K_{33}=2.0 \times 10^{-11} \text{ N}$, $K_{22}=1.0 \times 10^{-11} \text{ N}$, and rotational viscosity coefficient $\gamma=50 \text{ cp}$. The twisting rate and polar angle in the transition in the cell with homogeneous anchoring are shown in Figs. 2(a) and (b), respectively. In the beginning of the relaxation, the polar angle is $\pi/2$ at the surfaces and is 0 in bulk. The transition appears starting from the two surfaces and then propagating rapidly into the bulk. Detailed investigation reveals that the relaxation takes place everywhere in the cell. Near the surface, the initial polar angle is large and the relaxation is fast. In the middle of the cell, the initial polar angle is small (given by some random noise) and the relaxation is slow. The relaxation starting from the surface propagates into the bulk so quickly that the relaxation starting from the noise in the bulk is difficult to see. This propagation of the transition is not a diffusion process as in a homogeneous nematic cell where the dynamic equation for the polar angle θ is a diffusion equation. In the cholesteric liquid crystal, the dynamic equation for θ has a diffusion term and a nonlinear term. The nonlinear term makes the relaxation propagate quickly into the bulk. The liquid crystal relaxes to the transient planar texture (with $S=0.6$ and $\theta=\pi/2$) in about 1 ms. The average twisting rate and polar angle as a function of time are shown in Figs. 4(a) and (b), respectively.

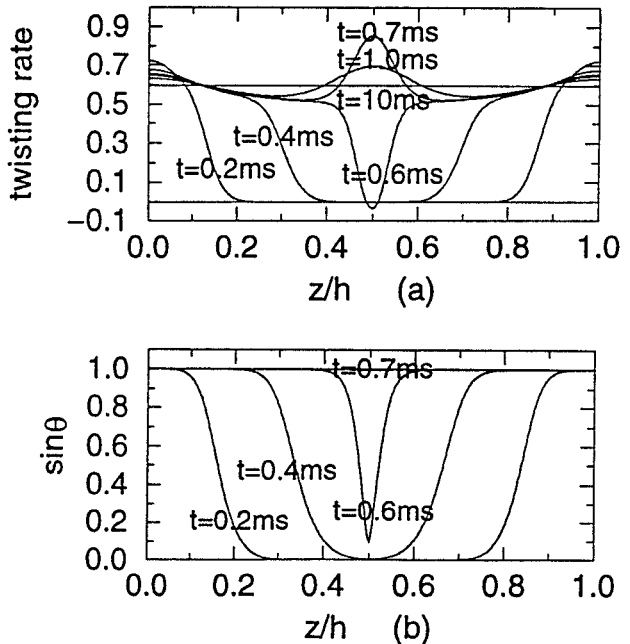


Fig. 2 Spatial dependence of the twist rate and polar angle at various times in the homeotropic-planar transition in the cell with homogeneous anchoring.

The twisting rate and polar angle in the transition in the cell with homeotropic anchoring are shown in Figs. 3(a) and (b), respectively. In the beginning of the relaxation, the polar angle is 0 at the surfaces and very small in bulk. The transition starts in the bulk and propagates to the two surfaces. In this stage of the relaxation, the twisting rate is larger in the middle than near the surface. The liquid crystal relaxes to the transient planar texture (with $S=0.5$ and $\theta=\pi/2$) in about 1.3 ms. The relaxation continues and the twisting rate keeps increasing. In this stage of the transition, the twisting rate is larger near the surface than in the middle. The helical structure is "injected" from the surfaces into the bulk. The liquid crystal relaxes to the stable planar texture (with $S=0.95$ and $\theta=\pi/2$) in about 30 ms. Therefore in this cell, the liquid crystal can relax directly to the stable planar texture without the nucleations required in the cell with homogeneous anchoring. The average twisting rate and polar angle as a function of time are shown in Figs. 4(a) and (b), respectively. The fast homeotropic-planar transition time in the cell with homeotropic anchoring is consistent with experimental results.⁵

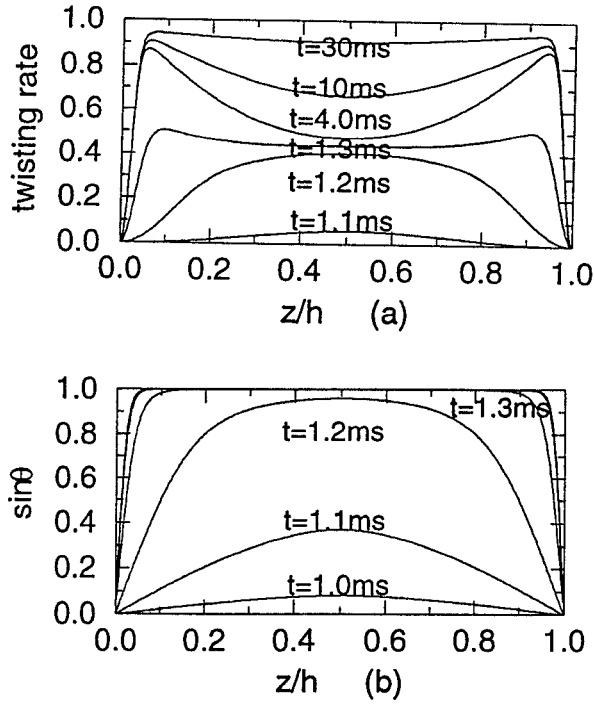


Fig. 3 Spatial dependence of the twist rate and polar angle at various times in the homeotropic-planar transition in the cell with homeotropic anchoring.

We also study effects of bias fields on the homeotropic-planar transition. We find that there is a critical field E_{hp} above which the applied bias field

creates an energy barrier and makes the transition impossible. This critical field E_{hp} depends on both cell thickness and surface anchoring; the result of our simulation is shown in Fig. 5. For the cell with homogeneous anchoring, the critical field vs. h/P_0 is shown by curve (a). The homogeneous anchoring favors the transient planar texture, and therefore the critical field is higher. As the cell thickness is increased, the critical field decreases and approaches the ultimate value of $0.6E_c$. For the cell with homeotropic anchoring, the critical field vs. h/P_0 is shown by curve (b). The homeotropic anchoring favors the homeotropic texture, and therefore the critical field is lower. As the cell thickness is increased, the critical field increases and approaches the ultimate value of $0.45E_c$.

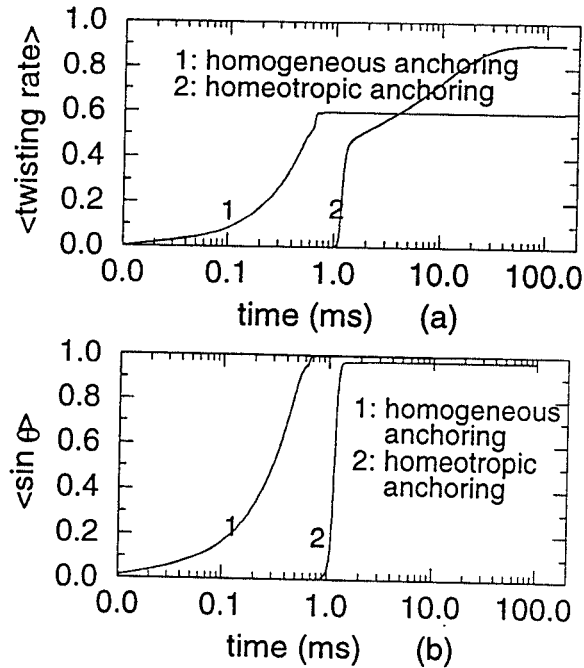


Fig. 4 Average twisting rate and polar angle vs. time.

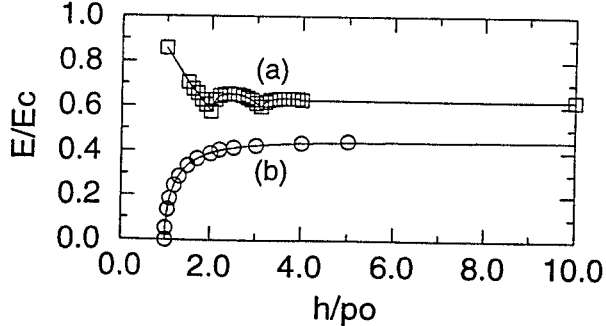


Fig. 5 The critical field of the homeotropic-planar transition vs. cell thickness. (a) the cell with homogeneous anchoring, (b) the cell with homeotropic anchoring.

In the cell with homogeneous anchoring, the relaxation from the transient planar texture to the stable planar texture is also affected by the applied bias field. The twisting rate as a function of time at various bias fields is plotted in Fig. 6. When the bias field is 0, the liquid crystal relaxes from the homeotropic texture to the transient planar texture (with the twisting rate of 0.6 and polar angle of $\pi/2$) in about 1 ms. Afterward, the twisting rate remains at 0.6. As discussed before, the liquid crystal cannot relax to the stable planar texture without nucleations from defects. As the bias field is increased, the relaxation from the homeotropic texture to the transient planar texture becomes slower. When the bias field is $0.5E_c$, the liquid crystal relaxes from the homeotropic texture to the transient planar texture (with the twisting rate of 0.7 and polar angle of $\pi/2$) in about 2 ms. Afterward, it remains in the transient planar texture. When the bias field is $0.6E_c$, the liquid crystal relaxes to the planar texture with twisting rate of 0.9, which is close to the intrinsic twisting rate of 1.0, in about 9 ms. This may be important in practice in reducing the homeotropic-planar transition time in cholesteric display cells with homogeneous anchoring. When the bias field is $0.7E_c$, above the critical field of $0.62E_c$, the homeotropic-transient planar relaxation becomes impossible, and the twisting rate remains at 0.0. One point should be pointed out is that in practice, when the bias field is sufficiently high, the liquid crystal may transform from the homeotropic texture to the focal conic texture, instead of the planar texture, if the focal conic texture has a lower free energy. In our modelling, we do not consider this possibility.

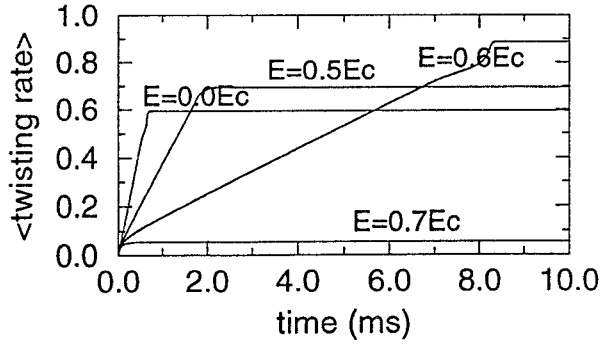


Fig. 6. Average twisting rate vs. time in the homeotropic-planar transition under various bias fields in the cell with homogeneous anchoring. $h/P_o = 10$.

The major parameters affecting the homeotropic-planar transition are the cell thickness h , elastic constant K_{22} and K_{33} , intrinsic pitch P_o and viscosity γ of the liquid crystal. The transition time is proportional to $\gamma P_o^2 / K_{22}$. Shorter transition time is achieved with

larger K_{22} and shorter pitch. In the cell with homogeneous anchoring, the cell thickness does not affect much the transition time. In the cell with homeotropic anchoring, however, the transition time depends on the cell thickness. Thinner cells will have shorter transition times. If K_{33} were equal to K_{22} , the liquid crystal would relax from the homeotropic texture to the planar texture directly, independent of the surface anchoring. In reality, K_{33}/K_{22} is always larger than 2; the ratio in that regime does not affect much the transition, nevertheless, a small ratio is preferred.

Conclusion

In an effort to understand the homeotropic-planar transition, we have done a numerical study of the transition using the tensor relaxation method. Our results show that in cells with homogeneous anchoring, the liquid crystal relaxes to the transient planar texture and remains there. The anchoring hinders continuous change of pitch. Further relaxation needs defects to serve as nucleation sites. The homeotropic-planar transition time is usually long. In cells with homeotropic anchoring, the helical structure can be "injected" from the surface, and the pitch can change continuously. The homeotropic-planar transition time is short, which explains the experimentally observed fast homeotropic-planar transition achieved in cells with homeotropic anchoring. Our study predicts that fast homeotropic-planar transition can also be achieved by applying a bias field in cells with homogeneous anchoring. This numerical study provides guide in choosing material parameters and designing display cells to optimize the performance of cholesteric reflective displays.

Acknowledgement

This research was supported in part by ARPA under contract number N61331-94-K-0042 and NSF under ALCOM grant number DMR89-20147. We wish to thank Prof. C. Gartland for useful discussions.

Reference

1. D.-K. Yang, J. L. West, L.C. Chien and J.W. Doane, *J. of Appl. Phys.*, **76**, p.1331 (1994).
2. D.-K. Yang, X.-Y. Huang and Y.-M. Zhu, *Annual Rev. Mater. Sci.*, **20**, p. 117 (1997).
3. X.-Y. Huang, D.-K. Yang, P. J. Bos, and J.W. Doane, *SID Dig. Tech. Papers*, p.347 (1995).
4. S. Dickmann, J. Eschler, O. Cossalter and D. A. Mlyniski, *SID Dig. Tech. Papers*, p. 638 (1993).
5. J. V. Gandhi, X.-D. Mi and D.-K. Yang, to be published in *Phys. Rev. E*, (1998). P. Watson, et al., *ALCOM Technical Report VIII*, 145 (1996).